

A-dependence of hadronization in nuclei

H.P. Blok^{1,2,*} and L. Lapikás^{2,†}

¹*Department of Physics and Astronomy, Vrije Universiteit, de Boelelaan 1081, 1081 HV Amsterdam, The Netherlands*

²*Nationaal Instituut voor Kernfysica en Hoge-Energie Fysica (NIKHEF), P.O. Box 41882, 1009 DB Amsterdam, The Netherlands*

(Dated: November 13, 2018)

The A -dependence of models for the attenuation of hadron production in semi-inclusive deep-inelastic scattering on a nucleus is investigated for realistic matter distributions. It is shown that the dependence for a pure partonic (absorption) mechanism is more complicated than a simple $A^{2/3}$ ($A^{1/3}$) behavior, commonly found when using rectangular or Gaussian distributions, but that the A -dependence may still be indicative for the dominant mechanism of hadronization.

PACS numbers: 13.60.Hb, 21.10.Gv, 25.30.Fj

The study of hadronization, the process that leads from partons produced in some elementary interaction to the hadrons observed experimentally, is of importance, both in its own right as a study of a non-perturbative QCD process, and in the interpretation of data from experiments that use outgoing hadrons as a tag. The end products of the hadronization process in free space are known from e^+e^- annihilation, but very little is known about the space-time development of the process. One way to investigate this is to study the semi-inclusive production of hadrons in deep-inelastic scattering of electrons from a nucleus, where the nucleus is used as a length(time)-scale probe (see Refs. [1, 2]).

Even if hadronization is not yet quantitatively understood, it is known that the following processes play a role in leptoproduction of hadrons in a nucleus (see also Fig. 1). After a quark in a nucleon is hit by the virtual photon, it loses energy by scattering from other quarks and radiating gluons, thus creating quark-antiquark pairs. After some time¹ and corresponding length l_f colorless (pre)hadrons² are formed. The average value L_f of the formation length has been estimated [3] based on the Lund model to be typically in the range of 1–10 fm if the virtual-photon energy is in the range 5–30 GeV. Hence, L_f is comparable to the size of a nucleus.

If the hadronization is fast, i.e., the hadrons are produced inside the nucleus, they can be absorbed, which will show up as an ‘attenuation’ of the hadron yield. (In experiments one measures the ratio R_A of the yield on a nucleus with mass number A and the one on a deuteron.) If, on the other hand, the hadronization is stretched out over distances large compared to the size of a nucleus,

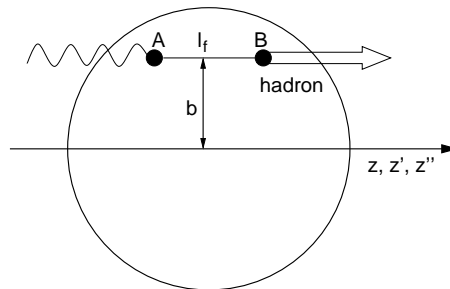


FIG. 1: Illustration of hadronization in a nucleus and used coordinates. The parton is produced at point A, while the hadron is formed at B. The distance l_f has a distribution with as average the formation length L_f .

the relevant interactions will be partonic, involving the emission of gluons and quark-gluon interactions, which also changes the production of hadrons.

Since hadronization, as a non-perturbative QCD process, cannot be calculated from first principles, various models have been developed (see, e.g., Refs. [4, 5, 6, 7, 8, 9]) to describe hadron production and attenuation in a nucleus. Some models focus on the partonic part, while others include or emphasize the hadronic part. In all cases a sizable dependence on the mass number A is predicted. However, often the calculations use simple forms for the matter distribution of the nucleus.

In this Report we investigate the A -dependence using realistic matter distributions. We will do this for two schematic models, covering the extremes sketched above. The first one (called model I) assumes a purely partonic mechanism, hadronization occurring outside of the nucleus (point B in Fig. 1 effectively at infinity) and thus absorption of the produced hadrons playing no role. The nuclear attenuation is then caused by the energy loss of the produced quark due to multiple scattering and gluon bremsstrahlung, which gives rise to a change of the hadron fragmentation function and thus to nuclear attenuation. Because of the Landau-Pomeranchuk-Migdal interference effect [10] this energy loss depends quadratically on the length of matter traversed by the hit quark

*Electronic address: henkb@nikhef.nl

†Electronic address: louk@nikhef.nl

¹ For a more detailed discussion of the concept of formation time etc. see Ref. [3].

² For the present discussion it is not needed to discriminate between hadrons and prehadrons, so in the remainder we will just talk about hadrons (but see, e.g., Refs. [4, 5]).

(for the present discussion we neglect contributions from other quarks; see Refs. [6, 7] for more details). In terms of the picture of Fig. 1 it depends on the square of the density-averaged distance the parton travels within the nucleus from the point where it is created (point A in Fig. 1).

On the other hand our second schematic model (called model II) assumes that a possible attenuation is completely due to absorption of the produced hadron, so nothing happens between the time the parton is produced and the hadron is formed (points A and B in Fig. 1). In a Glauber approach this attenuation depends on the cross section for absorption of the hadron³ and the density-averaged distance the hadron travels through the nucleus after it has been formed (see Fig. 1). Taking the absorption cross section to be constant (and small enough that a linear approximation is sufficient), the latter determines the nuclear attenuation.

This means we have to calculate the following two integrals:

$$\langle t_I^2 \rangle = \frac{2\pi}{A} \int_0^\infty b db \int_{-\infty}^\infty dz \rho_A(b, z) \left[\int_z^\infty dz' \rho_A(b, z') \right]^2, \quad (\text{model I}) \quad (1)$$

$$\langle t_{II} \rangle = \frac{2\pi}{A} \int_0^\infty b db \int_{-\infty}^\infty dz \rho_A(b, z) \int_z^\infty dz' L_f^{-1} e^{-(z'-z)/L_f} \int_{z'}^\infty dz'' \rho_A(b, z''). \quad (\text{model II}) \quad (2)$$

Here the exponential models the distribution of the formation distances l_f , and the matter densities ρ_A are normalized to A . (By entering these quantities with corresponding dynamical factors into the appropriate formula's of the models, hadron production cross sections and from these values for the attenuation R_A can be calculated. However, here we are interested in the A -dependence (and moreover the used models are extreme and schematic). Under the assumption that the cross section is linear in $\langle t_I^2 \rangle$ and $\langle t_{II} \rangle$, which is a good first-order approximation, the A -dependence of these quantities carries over into the one of the cross sections.)

It can easily be shown that for a nucleus with a mass density distribution described by one scale parameter, as in the case of a rectangular (as in the liquid-drop model) or a Gaussian distribution, the value of $\langle t_I^2 \rangle$ is proportional to the equivalent radius or rms radius squared, which in those cases leads to an $A^{2/3}$ dependence. In case of model II one finds for $\langle t_{II} \rangle$ for a rectangular distribution an $A^{1/3}$ dependence when $L_f = 0$, and a larger

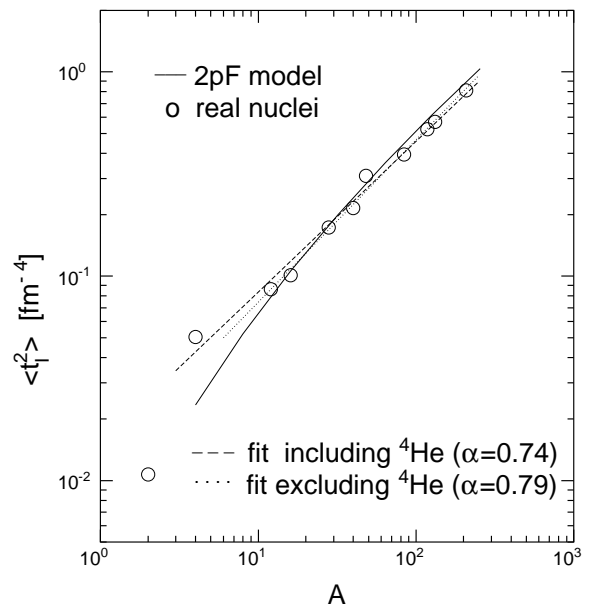


FIG. 2: Values of $\langle t_I^2 \rangle$ as function of A for 2-parameter Fermi (2pF) matter distributions (solid curve) and for actual nuclei (circles). The dashed line is a power-law (A^α) fit to the latter, excluding the point for the deuteron. The dotted line in addition excludes the point for ${}^4\text{He}$ in the fit.

exponent⁴ (e.g., about 0.55 for $L_f = 4$ fm) at larger L_f , and similar for a Gaussian distribution.

However, neither a rectangular nor a Gaussian distribution is a good representation of the mass distribution of a real nucleus. Therefore we have evaluated $\langle t_I^2 \rangle$ and $\langle t_{II} \rangle$ for a more realistic distribution, described by a 2-parameter Fermi (Saxon-Woods) form

$$\rho_A(r) = \rho_0 / [1 + e^{-(r-c)/a}] \quad (3)$$

with parameters $\rho_0 = 0.170$ nucleons/fm³, $a = 0.5$ fm, and the value of c so as to give a nucleus with A nucleons. (This form gives a reasonably good global description of the mass distribution down to low values of A). The results are given in Table I and are shown in Figs. 2 and 3.

It can be seen from Fig. 2 that for a 2pF matter distribution the A -dependence of $\langle t_I^2 \rangle$ is rather steep. If one tries to describe it with the power law A^α , it would require a value of α well in excess of $2/3$. Fig. 3 shows for the case of model II that the slope of the curve, in essence the value of α , increases when L_f increases. Values range from about $\alpha = 0.40$ for $L_f = 0$ fm to $\alpha = 0.60$ for $L_f = 4$ fm.

Given these findings, and since it is known that the parameters for actual nuclei are slightly irregular due to, e.g., shell closures, it is interesting to see the behavior of

³ In our simple model we do not take into account coupled-channels processes. Possible effects of these are discussed in Ref. [5].

⁴ This effect of taking into account a distribution of formation distances has been noted already in Ref. [8].

TABLE I: Values of $\langle t_I^2 \rangle$ and $\langle t_{II} \rangle$ for nuclei of mass number A , calculated with a 2pF distribution (see Eq. 3) with half radius c (second column) and $\rho_0 = 0.170 \text{ fm}^{-3}$ and $a = 0.5 \text{ fm}$ fixed. The values of $\langle t_{II} \rangle$ were calculated for five different values of L_f (columns 4–8).

A	c [fm]	$\langle t_I^2 \rangle$ [fm ⁻⁴]	$\langle t_{II} \rangle$ [fm ⁻²]				
			L_f [fm]				
			0.0	1.0	2.0	3.0	4.0
4	1.321	0.023	0.108	0.070	0.048	0.037	0.030
8	1.875	0.052	0.166	0.113	0.081	0.062	0.051
16	2.531	0.106	0.243	0.175	0.129	0.101	0.083
32	3.324	0.200	0.342	0.260	0.199	0.159	0.132
64	4.295	0.359	0.468	0.373	0.295	0.242	0.204
125	5.452	0.609	0.619	0.513	0.421	0.353	0.303
254	6.976	1.037	0.818	0.703	0.597	0.513	0.448

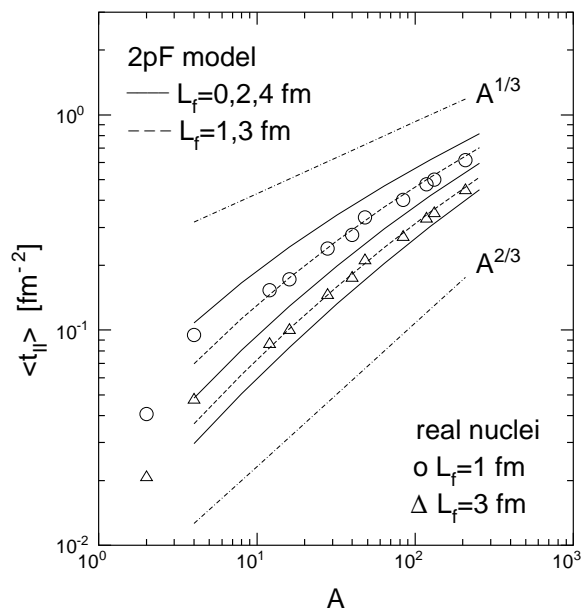


FIG. 3: Values of $\langle t_{II} \rangle$ as function of A for $L_f = 0, 2, 4 \text{ fm}$ (solid curves, top to bottom) and $L_f = 1, 3 \text{ fm}$ (dashed curves, top to bottom) for 2pF matter distributions and for actual nuclei (symbols) for $L_f = 1, 3 \text{ fm}$ only. The dot-dashed lines represent (arbitrarily normalized) $A^{1/3}$ and $A^{2/3}$ behaviors, as indicated.

$\langle t_I^2 \rangle$ and $\langle t_{II} \rangle$ for real nuclei, since those are used in experiments. For that purpose we have used parameterizations [11, 12] of measured charge distributions (since the neutron distribution is very similar the error introduced by using the charge distribution instead of the matter distribution is small, and irrelevant for the conclusions of the present study) for the nuclei ${}^2\text{H}$, ${}^4\text{He}$, ${}^{12}\text{C}$, ${}^{16}\text{O}$, ${}^{28}\text{Si}$, ${}^{40}\text{Ca}$, ${}^{48}\text{Ca}$, ${}^{84}\text{Kr}$, ${}^{118}\text{Sn}$, ${}^{132}\text{Xe}$ and ${}^{208}\text{Pb}$. The results are also given in Table II and shown as the symbols in Figs. 2 and 3.

TABLE II: Calculated values of $\langle t_I^2 \rangle$ and $\langle t_{II} \rangle$ for various nuclei. The rms radii of the employed mass distributions are given in the second column. The values of $\langle t_{II} \rangle$ were calculated for five different values of L_f (columns 4–8).

nucleus	r_{rms} [fm]	$\langle t_I^2 \rangle$ [fm ⁻⁴]	$\langle t_{II} \rangle$ [fm ⁻²]				
			L_f [fm]				
			0.0	1.0	2.0	3.0	4.0
${}^2\text{H}$	2.13	0.011	0.068	0.041	0.027	0.021	0.017
${}^4\text{He}$	1.72	0.050	0.159	0.095	0.063	0.047	0.038
${}^{12}\text{C}$	2.45	0.086	0.218	0.153	0.111	0.086	0.070
${}^{16}\text{O}$	2.73	0.101	0.238	0.172	0.127	0.100	0.082
${}^{28}\text{Si}$	3.08	0.173	0.316	0.239	0.181	0.145	0.120
${}^{40}\text{Ca}$	3.48	0.216	0.356	0.277	0.215	0.174	0.146
${}^{48}\text{Ca}$	3.47	0.309	0.428	0.333	0.259	0.210	0.175
${}^{84}\text{Kr}$	4.25	0.395	0.493	0.403	0.325	0.270	0.230
${}^{118}\text{Sn}$	4.67	0.523	0.571	0.475	0.390	0.328	0.281
${}^{132}\text{Xe}$	4.83	0.570	0.598	0.500	0.413	0.348	0.300
${}^{208}\text{Pb}$	5.51	0.811	0.719	0.615	0.519	0.445	0.387

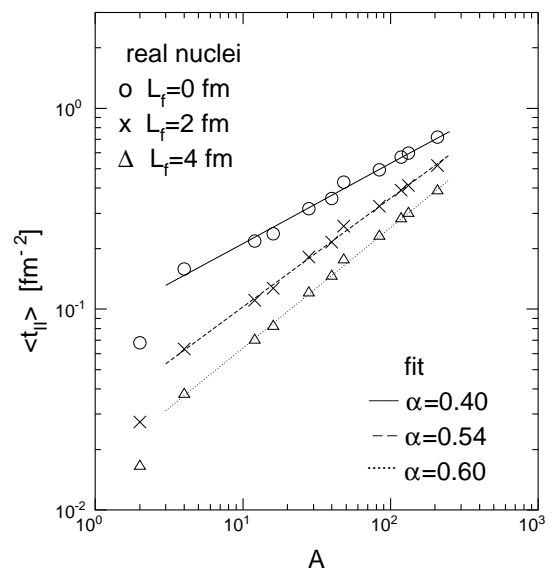


FIG. 4: Values of $\langle t_{II} \rangle$ as function of A for $L_f = 0, 2, 4 \text{ fm}$ for actual nuclei (symbols). The lines are results of power-law (A^α) fits, excluding the point for the deuteron.

A first observation is that while the results for $A \geq 4$ scatter around the global curve, the results for ${}^2\text{H}$ are way down. This is due to ${}^2\text{H}$ being a rather dilute system. Furthermore, it is seen that the results for ${}^4\text{He}$ lie slightly above the global curve, which is related to ${}^4\text{He}$ being a relatively dense system. Fitting the A -dependence of the results for the real nuclei including ${}^4\text{He}$ (but leaving out ${}^2\text{H}$), one finds an exponent of 0.74 for $\langle t_I^2 \rangle$ (see Fig. 2) and values between 0.40 and 0.60 for $\langle t_{II} \rangle$ depending on the value of L_f (see fig. 4). When ${}^4\text{He}$ is not included in the fit, the values of α in case of $\langle t_{II} \rangle$ change by less than

0.02, whereas in case of $\langle t_7^2 \rangle$ the value of α increases from 0.74 to 0.79. Thus, in trying to extract an A -dependence from experimental data it matters if one uses ${}^4\text{He}$ as lowest A nucleus, or, *e.g.*, ${}^{12}\text{C}$.

Given these results it would in principle be possible to discriminate on account of the A -dependence between the two extreme mechanisms that we have used here. However, in practice the process of hadronization in a nucleus most probably will be a combination of these mechanisms, with possibly even different dependences on path lengths in the nucleus than employed here. But whatever the mechanism, the A -dependence will be an important ingredient. Our results show that in model calculations of the A -dependence for comparison with experimental data, global mass distributions, such as a rectangular distribution employed in the liquid-drop model, are not

adequate. Instead, the use of experimentally established density functions for the nuclei actually used in the experiment is essential, where it even matters whether ${}^4\text{He}$ with its relatively large density is included or not.

Acknowledgments

One of us (HPB) likes to thank Dr. H. J. Pirner for useful discussions. We thank Dr. J. J. M. Steijger and Dr. G. van der Steenhoven for critically reading the manuscript. This work is part of the research program of the Stichting voor Fundamenteel Onderzoek der Materie (FOM).

-
- [1] A. Airapetian *et al.*, Eur. Phys. J. **C 20**, 479 (2001).
 - [2] A. Airapetian *et al.*, Phys. Lett. **B 577**, 37 (2003).
 - [3] A. Bialas and M. Gyulassy, Nucl. Phys. **B291**, 793 (1987).
 - [4] B. Z. Kopeliovich, J. Nemchik, E. Predazzi, and A. Hayashigaki, Nucl.Phys. **A740**, 211 (2004).
 - [5] T. Falter, W. Cassing, K. Gallmeister, and U. Mosel, Phys. Rev. C **70**, 054609 (2004).
 - [6] E. Wang and X.-N. Wang, Phys. Rev. Lett. **89**, 162301 (2002).
 - [7] F. Arleo, Eur. Phys. J. **C30**, 213 (2003).
 - [8] A. Accardi, D. Grünwald, V. Muccifora, and H. J. Pirner, Nucl. Phys. **A761**, 67 (2005); Erratum: hep-ph/0508036.
 - [9] A. Accardi, Acta Phys. Hung. to be published; nucl-th/0510090.
 - [10] L. D. Landau, I. Ya. Pomeranchuk, Dokl. Akad. Nauk SSSR **92**, 535 (1953); A. B. Migdal, Phys. Rev. **103**, 1811 (1956).
 - [11] H. de Vries, C. W. de Jager, and C. de Vries, Atom. Data and Nucl. Data Tables **36**, 495 (1987).
 - [12] G. Fricke, C. Bernhardt, K. Helig, L. A. Schaller, L. Schellenberg, E. B. Shera, and C. W. de Jager, Atom. Data and Nucl. Data Tables **60**,177 (1995).